Resilient Distributed Antenna System via Dynamic Cell-Restructuring

Sijie Xia*, Suguru Kameda*, Qiang Chen†‡, and Fumiyuki Adachi‡
*Research Institute for Semiconductor Engineering, Hiroshima University
1-4-2 Kagamiyama, Higashi-Hiroshima, Hiroshima, 739-8527 Japan
†Department of Communications Engineering, Graduate School of Engineering, Tohoku University
6-6-05 Aza-Aoba, Aramaki, Aoba-ku, Sendai, Miyagi, 980-8579 Japan
‡International Research Institute of Disaster Science, Tohoku University
468-1 Aoba, Aramaki, Aoba-ku, Sendai, Miyagi, 980-8572, Japan
E-mail: {xiasijie, kameda3}@hiroshima-u.ac.jp, {qiang.chen.a5, fumiyuki.adachi.b4}@tohoku.ac.jp

***Abstract*—This paper presents a resilient multi-cell distributed antenna system (DAS) capable of reconfiguring user–clusters and cell structures after antenna failure. A constrained K-means algorithm is employed to jointly optimize user-clustering, ensuring balanced load and effective antenna sharing under various antenna failure conditions. Two types of cell-restructuring are considered: a fixed-cell-number (FCN) approach that keeps the number of cells constant, and a variable-cell-number (VCN) approach that reduces the total number of cells compared with the normal state. Simulation results demonstrate that, even with a 50% antenna failure ratio, the proposed multi-cell DAS recovers over 40% of the original link capacity for the worst 1% users by cell-restructuring.**

***Index Terms*—Distributed antenna system (DAS), disaster resilience, clustering, cell-restructuring**

I. Introduction

Large-scale natural disasters such as earthquakes, hurricanes, and floods can severely damage radio access infrastructures, including base stations (BSs), mobile fronthaul, and power supply. Such failures often lead to significant communication service degradation and long network recovery times. Distributed antenna system (DAS) or cell-free system has emerged as a promising architecture for enhancing coverage and reliability [1]. By deploying multiple low-power distributed antennas (hereafter, antennas) across a wide area, DAS achieves improved communication quality through spatial diversity compared with conventional co-located antenna arrays [2], [3], especially when a higher frequency band such as mmWave band is utilized.

Despite these benefits, conventional DAS architectures rely on static cell boundaries and fixed user–antenna associations, which become inefficient under disaster-induced failures. When a subset of antennas or fronthaul connections becomes unavailable, the original cell configuration can lead to severe load imbalance and coverage gaps. Prior studies on disaster-resilient radio access networks (RANs) highlight that rapid connectivity restoration requires flexible and adaptive resource reconfiguration rather than depending solely on static redundancy [4]. In addition, recent surveys on post-disaster communications and public-safety wireless systems emphasize the necessity of dynamically reallocating and restructuring access-layer resources to maintain service continuity under infrastructure damage [5], [6]. These insights collectively indicate that a disaster-resilient RAN must incorporate algorithmic reconfiguration capabilities to adapt its topology to the spatial distribution of surviving antennas.

To address these challenges, this paper investigates a multi-cell DAS architecture capable of adaptive user-clustering and cell-restructuring after antenna failures. In the proposed multi-cell DAS, multiple BSs are deployed over a wide communication service area, with each BS controlling antennas within a sub-area called a cell. Within each cell, users are grouped exclusively into user-clusters, while antennas are shared between clusters and temporarily deactivated to save energy. We formulate a joint user–antenna clustering problem that considers large-scale channel gains and damage-aware constraints, and integrate it with a dynamic cell-restructuring framework: (i) fixed-cell-number (FCN) approach that keeps the number of cells constant by reducing the number of antennas in each cell, and (ii) variable-cell-number (VCN) approach that keeps the number of antennas per cell approximately constant by reducing the total number of cells compared with the normal state. This design concept follows the principle of "connect first, optimize later," ensuring continuity of service while gradually improving system efficiency.

Existing works on DAS clustering mainly address steady-state interference coordination [2], [3], whereas disaster recovery frameworks focus on high-level RAN self-organization without explicit modeling of antenna failures. UAV-assisted approaches [7] can improve resilience but require additional airborne or mobile infrastructure. In contrast, our approach performs internal topology reconfiguration within a ground-based DAS, providing a scalable and infrastructure-independent solution.

The main contributions are summarized as follows: (1) A disaster-aware joint user–antenna clustering formulation for multi-cell DAS that ensures fair user experience and

979-8-3315-7111-5/26/$31.00

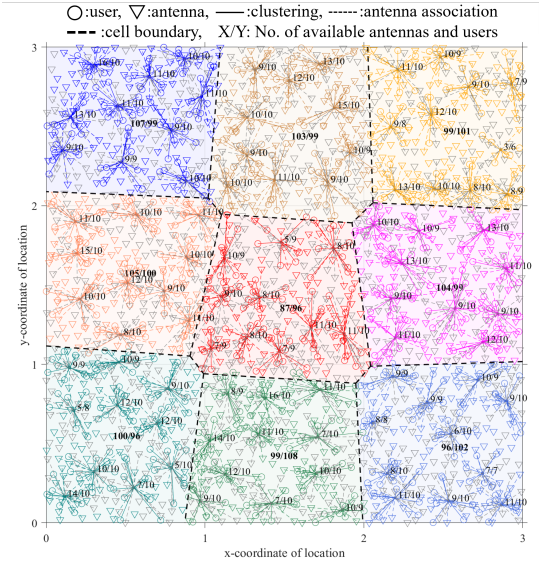

Fig. 1: An example of multi-cell DAS after antenna failure.

suppresses inter-cluster interference under antenna failure constraints. (2) A dynamic cell reconstruction mechanism operating in both fixed-cell and variable-cell modes, enabling rapid capacity recovery using surviving antennas.

The remainder of this paper is organized as follows. Section II describes the system model of the multi-cell DAS under disaster conditions. Section III describes the proposed joint user–antenna clustering and cell-restructuring method. Section IV presents the simulation results under various antenna failure scenarios. Section V concludes the paper.

II. System Model

Without loss of generality, we consider a multi-cell DAS deployed over a normalized square-shaped communication service area with an integer edge length $\sqrt{N}$, which can represent any physical scale, where N denotes the number of BSs deployed over the area. The coverage area of each BS is called the cell. A antennas are deployed over the service area to serve U single-antenna users. Each of the N BSs is connected to the distributed antennas within its own cell via optical mobile fronthaul.

Users and antennas are randomly distributed in the area. Within each cell, several user-clusters are dynamically formed to perform cluster-wise multi-user multiple-input multiple-output (MU-MIMO) transmission and reception, according to user distribution. The cell and cluster structure and their reconfiguration strategies will be described in Section III. Here, we focus on modeling the signal transmission procedure in the multi-cell DAS environment. The multi-cell DAS operates in time-division duplexing (TDD) mode, assuming channel reciprocity between uplink and downlink transmissions.

A. Disaster Model

In the normal state, all antennas are active and jointly serve the users in each cell. If some antennas become disabled due to a disaster, partial loss of coverage or user capacity degradation may occur. In this paper, for simplicity, we consider only antenna failure, while assuming that all BSs remain operational. Denoting the antenna failure ratio as ρ_{f}, the total number of active antennas to serve users decreases to $A' = (1-\rho_{\mathrm{f}})\,A$. The active antenna set for the whole system is denoted by $\mathcal{A}'$. One example of cell and cluster structure after antenna failure is shown in Fig. 1. Different colors distinguish the cells, where users and active antennas are connected to their corresponding cluster centers to indicate their associations. Gray triangles represent failed antennas. The numbers shown at each cell/cluster center denote the "available antennas/users" within that region.

B. Channel and Transmission Model

Considering the downlink transmission, the received signal is expressed for user u in cluster k of cell n as

$$y_u = \sqrt{P}\,\mathbf{h}_{u,k,n}^H \mathbf{w}_u s_u + \sum_{v\in\mathcal{U}_{k,n},\, v\neq u} \sqrt{P}\,\mathbf{h}_{u,k,n}^H \mathbf{w}_v s_v + \sum_{v\in\mathcal{U}_{j,m},\, j\neq k,\, m\neq n} \sqrt{P}\,\mathbf{h}_{u,j,m}^H \mathbf{w}_v s_v + n_u, \tag{1}$$

where $\mathbf{h}_{u,k,n}^H \in \mathbb{C}^{1\times A_{k,n}}$, $\mathbf{w}_u \in \mathbb{C}^{A_{k,n}\times 1}$, and n_u are respectively the precoding weight vector of user u, the channel gain vector between user u and antennas in the cluster j of the cell m, and the noise component characterized by zero-mean complex Gaussian random variable with variance 1 for user u. P is the normalized transmit signal-to-noise ratio (SNR), which is defined as the received SNR when the transmitter-receiver distance is equal to the normalized length 1 and is assumed to be same for all users. s_u is the transmit data symbol with unit variance for user u. The channel gain between each user and antenna is modeled as a composite of distance-dependent path loss, log-normal shadowing, and Rayleigh fading. In (1), the second and third terms correspond to the inter-user interference (IUI) within the same cluster and the inter-cluster interference (ICI) from other clusters inside and outside the same cell, respectively.

The partial interference-suppression multi-user zero-forcing (IS-MU-ZF) precoding [8] is employed to mitigate both IUI and ICI within the same cell. It is assumed that the channel state information (CSI) between all users and all antennas in each cell is perfectly known at the transmitter (BSs in downlink). The precoding follows a ZF scheme based on pseudo-inversion of the effective channel matrix. Accordingly, the precoding weight vector for user u in cluster k of cell n is given by

$$\mathbf{w}_u = \frac{\mathbf{v}_u}{\|\mathbf{v}_u\|}, \quad \mathbf{v}_u = \mathbf{h}_{u,k,n}^H \left(\sum_{v\in\mathcal{U}_n} \mathbf{h}_{v,k,n} \mathbf{h}_{v,k,n}^H \right)^{\dagger}. \tag{2}$$

and $\mathcal{U}_n$ denotes the set of users in cell n whose interference is suppressed by the given transmission scenario. Based on this,

the downlink user capacity of user u can be computed by

$$C_u = \log_2\left(1 + \frac{P\,|\mathbf{h}_{u,k,n}^H \mathbf{w}_u|^2}{\sum_{v\in\mathcal{U}_{j,m},\, v\neq u} P\,|\mathbf{h}_{u,j,m}^H \mathbf{w}_v|^2 + 1}\right). \quad (3)$$

III. Proposed Dynamic Clustering and Cell-Restructuring Methods

In the proposed multi-cell DAS, the cells consisting of distributed antennas are pre-defined according to their geographical deployment. Each user is then associated with the cell that contains the nearest active antenna. After this initial user-cell association, user–clusters are dynamically formed within each cell to perform cluster-wise MU-MIMO. The following subsections describe the proposed clustering and the subsequent cell restructuring procedures in detail.

A. Constrained K-Means-Based Clustering

The K-means algorithm [9] is a well-established and computationally efficient clustering method that can be effectively applied to location-based scenarios. In our multi-cell DAS, it is used to group neighboring users into clusters, allowing each cluster to perform ZF-based MU-MIMO to eliminate the intra-cluster IUI. However, conventional ZF or other matrix-inversion-based schemes entail computational complexity proportional to the cube of the number of users and/or antennas participating in MU-MIMO operations [10]. Consequently, uneven cluster sizes lead to unbalanced computational loads and degraded overall efficiency.

To address this issue, we employ a constrained K-means algorithm that limits the maximum cluster size T_{cls}, thereby ensuring that all clusters have relatively balanced sizes [11]. This approach not only maintains fairness in computational demand across clusters but also stabilizes the overall system complexity. The number of clusters within cell n is given by $K_n = \lceil U_n / T_{\text{cls}} \rceil$, where U_n denotes the total number of users in cell n. As a result, the user clustering is formulated as an integer programming problem in (4), which is iteratively solved until the clustering results no longer change. Here, $\mathbf{x}_u$, $\mathbf{x}_k$, and $I_{u,k}$ denote the coordinate of user u, the coordinate of cluster k (initially selected from user locations), and the association indicator between user u and cluster k, respectively.

$$\min_{\{I_{u,k}\}} \quad \sum_{u=1}^{U_n}\sum_{k=1}^{K_n} I_{u,k}\cdot\|\mathbf{x}_u - \mathbf{x}_k\|^2$$
$$\text{s.t.} \begin{cases} \sum_{u=1}^{U_n} I_{u,k} \le T_{\text{cls}},\ \forall k, \\ \sum_{k=1}^{K_n} I_{u,k} = 1,\ \forall u, \\ I_{u,k} = \begin{cases} 1, \text{association} \\ 0, \text{otherwise} \end{cases}. \end{cases} \quad (4)$$

For antenna association, also the distance-based criterion is applied in this paper. To ensure a fair user experience, an equal number N_a of antennas are associated with each user through a competitive association process. To maintain robustness under severe antenna failure conditions, any antenna is allowed to be associated with multiple clusters if the total number of active antennas becomes insufficient. To realize the competitive antenna association, we repeatedly solve the following integer program N_a times for each cluster individually, each time selecting one antenna per user and removing the selected antenna from that user's candidate antenna set.

$$\min_{\{I_{u,a}\}} \quad \sum_{u=1}^{U_n}\sum_{a\in\mathcal{A}'\setminus\mathcal{A}_{k,n}} I_{u,a}\left\|\mathbf{x}_u - \mathbf{x}_a\right\|^2$$
$$\text{s.t.} \begin{cases} \sum_{a\in\mathcal{A}'} I_{u,a} = 1, \quad \forall u, \\ I_{u,a} = \begin{cases} 1, & \text{association}, \\ 0, & \text{otherwise}, \end{cases} \end{cases} \quad (5)$$

where $\mathcal{A}_{k,n}$ is the antenna set associated with the cluster k in cell n. Although antenna sharing among different clusters may introduce additional ICI, such interference can be effectively suppressed by the IS-MU-ZF-based transmission scheme. In addition, as illustrated in Fig. 1, some antennas located far from all users (i.e., having weak large-scale channel gains) remain unassociated even in the normal state. These antennas can be temporarily deactivated to reduce unnecessary energy consumption, which is consistent with the disaster-resilient and energy-efficient design principles highlighted in Section I.

B. Constrained K-Means-Based Cell-Restructuring

The cell structure is also restructured using the constrained K-means algorithm from the perspective of computational complexity. In this stage, the clustering objective is applied to antennas instead of users, with a maximum cell size constraint, T_{cel}. As mentioned earlier, the number N of cells can be dynamically adjusted according to the total number of active antennas, as well as T_{cel}.

Under the normal state, each cell in the multi-cell DAS independently manages its antennas and users. However, under antenna failure conditions due to a disaster, the number of active antennas may decrease to A', resulting in capacity degradation. Therefore, it is necessary to reperform cell-restructuring as well as antenna-cluster reassociation. The constrained K-means-based method can be naturally extended to FCN and VCN approaches. The FCN approach keeps the total number N of cells by decreasing the number of antennas in each cell in proportion to the antenna failure ratio ρ_{f}, i.e., $A'_n \le T'_{\text{cel}} = (1-\rho_{\text{f}})T_{\text{cel}}$. This approach preserves the original cell numbers and similar coverage but sacrifices spatial diversity within each cell. On the other hand, the VCN approach keeps the number of antennas per cell approximately constant by decreasing the total number of cells compared with the normal state (i.e., $N' = \lceil A'/T_{\text{cel}} \rceil$). This approach merges adjacent cells having insufficient number of active antennas, thereby balancing both coverage and antenna utilization.

After cell-restructuring, the re-clustering process is performed to update user–antenna associations under the new cell topology. For comparison, Fig. 2 illustrates three approaches: (1) only antenna reassociation (OAR) without cell-

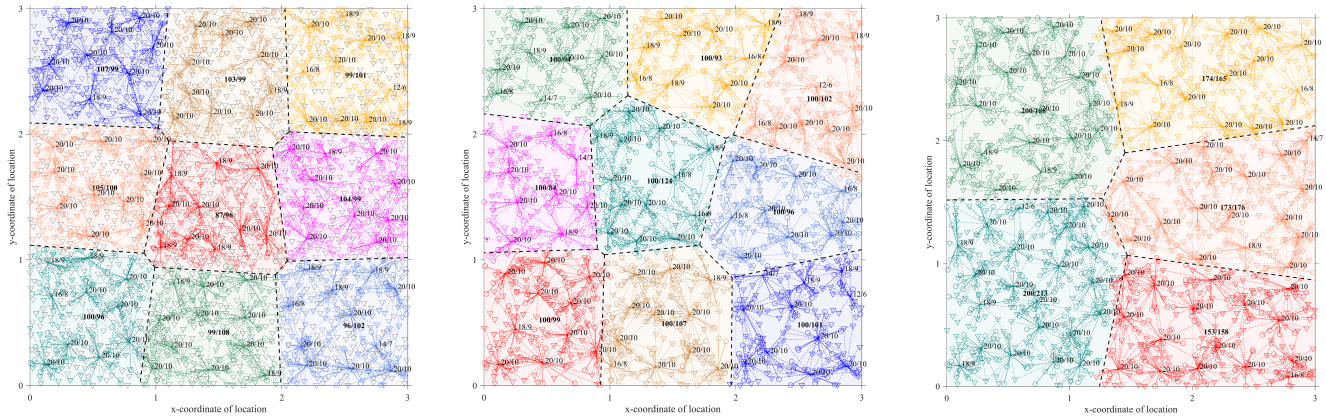

(a) OAR without cell-restructuring (b) FCN-based cell-restructuring (c) VCN-based cell-restructuring

Fig. 2: Cluster and cell restructuring results.

restructuring, (2) the FCN-based cell-restructuring, and (3) the VCN-based cell-restructuring. As observed, all of OAR, FCN, and VCN ensure that each cluster contains a sufficient number of antennas; however, their cluster layouts and antenna-reuse patterns differ significantly.

IV. Simulation Evaluation

In this section, computer simulations are conducted to evaluate the capacity performance achievable with OAR without cell-restructuring, FCN and VCN-based cell-restructurings. The simulation parameters are summarized in Table I. Specifically, a fixed antenna deployment pattern is generated once and shared across all simulation trials to ensure consistency. To emulate user mobility, user locations are randomly generated 1000 times, and for each of user location layout, independent shadowing and Rayleigh fading realizations are applied. For each user location layout, antenna failures are randomly imposed according to a given antenna damage ratio ρ_{f}. The resulting downlink capacities are then compared among five configurations: the normal case, the damaged case (without recovery), and three restructuring cases: OAR, FCN, and VCN.

Note that when a disaster occurs, the number of available antennas may fall below the number of users in a cluster. To ensure fair transmission opportunities, a round-robin scheduling scheme [12] is adopted to assign users randomly and evenly across time slots. The number of time slots required for each cluster is defined as $L_{k,n} = \lceil U_{k,n}/A'_{k,n} \rceil$, where $U_{k,n}$ and $A'_{k,n}$ denote the numbers of users and active antennas in cluster k of cell n, respectively.

In Fig. 3, the cumulative distribution functions (CDFs) of the downlink user capacities achieved by the proposed clustering and cell-restructuring approaches for the case of $\rho_{\mathrm{f}} = 50\%$. For reference, the CDF of the normal state is also plotted. Compared with the normal state, the capacity performance degrades significantly after antenna failures. The loss of coverage and spatial diversity, together with the additional scheduling overhead for time-domain user coordination, severely reduces the achievable user capacity.

TABLE I: Simulation settings

Parameter	Value
No. of antennas (A)	1800
No. of users (U)	900
Max no. of antennas in each cell (T_{cel})	200 (normal case)
Max no. of users in each cluster (T_{cls})	10
No. of antennas associated with each user (N_a)	2
Antenna damage ratio (ρ_{f})	10% $\sim$ 50%
Path loss exponent	3.5
Standard deviation of shadowing loss	8 dB
Normalized transmit SNR (P)	0 dB

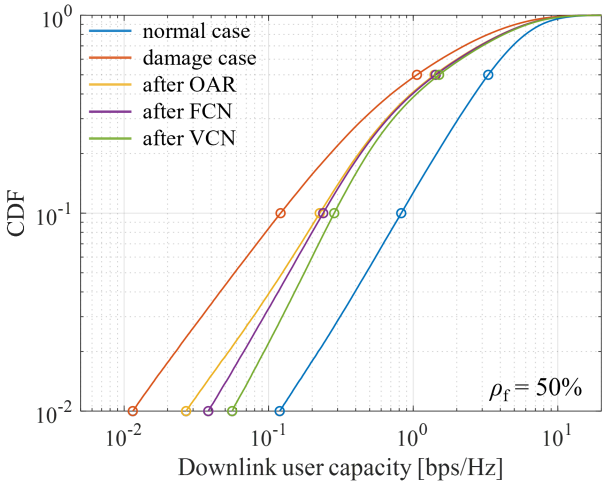

Fig. 3: CDF of downlink user capacity with $\rho_{\mathrm{f}} = 50\%$.

In contrast, the proposed restructuring approaches, i.e., FCN-based and VCN-based cell restructurings, provide substantial performance recovery compared with OAR, which does not involve cell restructuring. OAR fails to adapt the cluster and cell topology to the changed spatial distribution of available antennas, thereby offering only limited improvement. FCN achieves better performance by reorganizing cell bound-

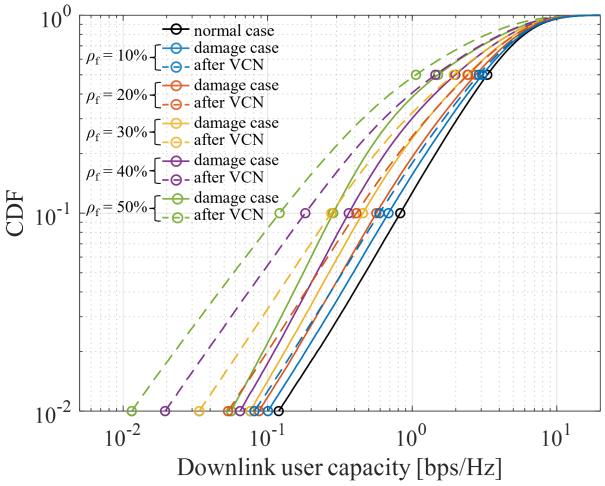

Fig. 4: CDF of downlink user capacity as a function of ρ_f.

aries; however, the reduced number of active antennas per cell limits its attainable spatial diversity. On the other hand, the VCN approach achieves the best performance among the three, as it preserves intra-cell spatial diversity while mitigating inter-cell ICI by reducing the total number of cells.

Nevertheless, the capacity achieved by VCN still remains below that in the normal state, primarily due to the increased path loss caused by enlarged cell areas and the severe ICI resulting from heavily reused antennas under antenna-scarce conditions. More specifically, the user capacity at CDF $=$ 0.01 (1%) decreases from 0.125 bps/Hz in the normal state to 0.012 bps/Hz after the disaster, but is improved to 0.057 bps/Hz by the proposed VCN approach, recovering approximately 40% of the lost capacity. These results demonstrate the effectiveness of the proposed restructuring approach in mitigating disaster-induced performance degradation. Since the uplink exhibits similar results, we omit them for brevity.

Then, Fig. 4 compares the CDFs of downlink user capacities for the normal case, the damaged case without cell-restructuring, and the proposed VCN-based cell-restructuring under various values of antenna failure ratios ρ_f. As expected, the capacity performance deteriorates with increasing ρ_f due to the more reduced number of active antennas.

Nevertheless, for all considered ρ_f values, the proposed VCN-based cell-restructuring consistently recovers a substantial portion of the lost capacity. In particular, the improvement in the lower-capacity region (e.g., CDF $<$ 0.1 (10%)) becomes more pronounced as the antenna failure ratio increases. This is due to the fact that users located in poorly covered areas benefit more from the flexible antenna re-association and adaptive cell merging inherent in the VCN approach. When $\rho_f = 10\%$, most users still can find nearby antennas, and the capacity recovery effect remains moderate. However, when $\rho_f = 50\%$, VCN dynamically expands cell boundaries and reassociates active antennas, thereby improving the user capacity, particularly for users near cell edges. The above results confirm that the proposed cell-restructuring effectively mitigates disaster-induced performance degradation and enhances overall network resilience.

V. Conclusions

In this paper, we proposed multi-cell DAS which reconfigures user–clusters and cell structures after antenna failure caused by disaster. The proposed cell-reconfiguration effectively adapts the cell and user-cluster structures to changes in the topology of active antennas, maintaining balanced computational complexity while improving capacity performance. Simulation results showed that, even under severe antenna failure conditions, the proposed cell-restructuring approaches, particularly the VCN-based cell-restructuring, can significantly improve the capacity, recovering around 40% of the loss compared with the normal state when $\rho_f = 50\%$. This confirms that the proposed cell-restructuring is effective for enhancing disaster resilience and maintaining communication service continuity.

Acknowledgment

This work was conducted under the commissioned research (No.02201) by National Institute of Information and Communications Technology (NICT), Japan, and was partially supported by the Japan Science and Technology Agency (JST) under the ASPIRE program (Grant Number JPMJAP2414).

References

[1] J. Zhang, S. Chen, Y. Lin, J. Zheng, B. Ai, and L. Hanzo, "Cell-free massive MIMO: A new next-generation paradigm," *IEEE Access*, vol. 7, pp. 99878–99888, 2019.

[2] D. Castanheira and A. Gameiro, "Distributed antenna system capacity scaling [coordinated and distributed MIMO]," *IEEE Wireless Commun.*, vol. 17, no. 3, pp. 68–75, Jun. 2010.

[3] L. Dai, "A comparative study on uplink sum capacity with co-located and distributed antennas," *IEEE J. Sel. Areas Commun.*, vol. 29, no. 6, pp. 1200–1213, Jun. 2011.

[4] T. Sakano *et al.*, "Disaster-resilient networking: A new vision based on movable and deployable resource units," *IEEE Netw.*, vol. 27, no. 4, pp. 40–46, Jul./Aug. 2013.

[5] M. Matracia, N. Saeed, M. A. Kishk, and M.-S. Alouini, "Post-disaster communications: Enabling technologies, architectures, and open challenges," *IEEE Open J. Commun. Soc.*, vol. 3, pp. 1177–1205, 2022.

[6] K. Ali, H. X. Nguyen, Q.-T. Vien, P. Shah, M. Raza, and V. V. Paranthaman, "Review and implementation of resilient public safety networks: 5G, IoT, and emerging technologies," *IEEE Netw.*, vol. 35, no. 2, pp. 18–25, Mar.-Apr. 2021.

[7] M. Matracia, M. A. Kishk, and M.-S. Alouini, "On the topological aspects of UAV-assisted post-disaster wireless communication networks," *IEEE Commun. Mag.*, vol. 59, no. 11, pp. 59–64, Nov. 2021.

[8] S. Xia, C. Ge, R. Takahashi, Q. Chen, and F. Adachi, "Adaptive interference suppressing multi-user ZF in cluster-centric cell-free massive MIMO systems," *IEEE Commun. Lett.*, vol. 28, no. 6, pp. 1422–1426, Jun. 2024.

[9] S. Lloyd, "Least squares quantization in PCM," *IEEE Trans. Inf. Theory*, vol. 28, no. 2, pp. 129–137, Mar. 1982.

[10] Q. H. Spencer, A. L. Swindlehurst, and M. Haardt, "Zero-forcing methods for downlink spatial multiplexing in multiuser MIMO channels," *IEEE Trans. Signal Process.*, vol. 52, no. 2, pp. 461–471, Feb. 2004.

[11] P. Bradley, K. Bennett, and A. Demiriz, "Constrained K-means clustering," Microsoft Research, Tech. Rep. MSR-TR-2000-65, May 2000.

[12] Y. Zhong, T. Q. S. Quek, and X. Ge, "Heterogeneous cellular networks with spatio-temporal traffic: Delay analysis and scheduling," *IEEE J. Sel. Areas Commun.*, vol. 35, no. 6, pp. 1373–1386, Jun. 2017.